Appl Phys B (2009) 94: 459–465
DOI 10.1007/s00340-008-3309-7

Applied Physics B
Lasers and Optics

Intensity-driven, laser induced transformation of Ag nanospheres to anisotropic shapes

A. Stalmashonak · A. Podlipensky · G. Seifert · H. Graener

Received: 31 July 2008 / Revised version: 30 October 2008 / Published online: 19 November 2008

Abstract The shapes of initially spherical Ag nanoparticles in soda-lime glass are persistently changed using fs laser irradiation. With linearly polarized pulses, this shape transformation of the nanoparticles causes optical dichroism of the material. The intensity dependence of this effect is studied comprehensively, addressing the whole intensity range of permanent modifications as well as the influence of the number of laser pulses applied to one spot on the sample. The results are used as basis to develop a complete scenario of the possible mechanisms leading to the laser-induced shape transformation of metallic nanoparticles in glass.

PACS 78.67.-n · 73.20.Mf

1 Introduction

Composite materials containing metal nanoparticles have been in the focus of extensive research efforts for several years because of their numerous potential applications in different fields of science and technology [1–3], such as novel nonlinear materials, nanodevices and optical elements. As linear and nonlinear optical properties of such nanocomposites are dominated by the Surface Plasmon Resonance (SPR) of the metal particles, the key parameters for tailoring their properties are size, shape, concentration, and spatial distribution of the nanoparticles, as well as the properties of the surrounding matrix. Laser-induced techniques represent a very powerful and flexible tool to control these parameters [4–15]. Particularly, it was discovered that initially spherical silver nanoparticles embedded in soda-lime glass experience a persisting transformation into ellipsoidal shape when irradiated with intense fs laser pulses at a wavelength near to the SP resonance [9–15]. Two regimes of irradiation leading to different shapes have been identified [14, 15]: (i) Applying successively many pulses at relatively low intensity on one spot (multi-shot mode), the initial nanospheres are transformed to prolate spheroids. (ii) Using higher intensity, but only one pulse per spot (single-shot regime), oblate spheroids are produced. In both cases the symmetry axes of the particles are oriented along the polarization vector of the laser light (briefly referred to as 'laser polarization' in the following) [15]. Also in both cases, heating of the samples for at least several minutes above the glass transition temperature (∼600°C in soda-lime glass) restores the original, non-dichroic optical extinction, i.e., obviously causes a reshaping of the nanoparticles to spheres [12, 14].

Our previous results showing common particle symmetry in the two irradiation regimes [15] represent only two points in the two-dimensional field of peak pulse intensity and number of pulses applied. For a still lacking comprehensive picture of the physical processes behind, however, the whole field of parameters has to be studied. In particular, the following questions in this context are still open: (i) Is there a single pulse intensity threshold for deformation, or can lower intensity be compensated by irradiating more pulses? (ii) At which intensity/number of pulses applied does the

A. Stalmashonak (✉) · A. Podlipensky · G. Seifert · H. Graener
Institut für Physik, Martin-Luther-Universität Halle-Wittenberg, Hoher Weg 8, 06120 Halle, Germany
e-mail: andrei.stalmashonak@physik.uni-halle.de
Fax: +49-345-5527034

Present address:
A. Podlipensky
Institute of Optics, Information and Photonics, Photonics & New Materials Research Group, University Erlangen-Nuernberg, Günther-Scharowsky-Str. 1/Bau 24, 91058 Erlangen, Germany

transition from prolate to oblate shape occur, and which particle shapes are produced there? (iii) What happens with the particles going to very high irradiation intensity and/or large number of pulses applied to one spot?

It is the intention of this paper to answer these questions. We will therefore show and analyze in detail novel results of irradiation experiments, where laser intensities and number of pulses applied to one spot comprise the whole range of reasonably observable laser induced dichroism.

2 Experiment

The samples used in our experiments were prepared using the Ag–Na ion exchange method for soda-lime float glass with following annealing in H_2 reduction atmosphere [16]. This technique results in the formation of spherical silver nanoparticles of 30 nm mean diameter in a thin surface layer of approximately 6 μm thickness. The volume filling factor of Ag nanoparticles decreases in the depth of the glass substrate [12]. By removing a well-defined surface layer by etching in 15% HF acid, samples with a silver volume fraction of about 0.001 were prepared. These samples are well-suited to study the photomodification of isolated, non-interacting nanoparticles.

The samples were irradiated by linearly polarized laser pulses from an amplified, frequency doubled Ti:Sapphire laser (wavelength $\lambda = 400$ nm, pulse duration $\tau_{FWHM} = 150$ fs, repetition rate 1 kHz). Focusing the laser beam onto the sample surface with a minimum beam size of ∼200 μm, a maximum laser peak pulse intensity of 4 TW/cm^2 was achieved, which is more than one order of magnitude below the typical breakdown threshold of transparent glass [17]. The applied irradiation density was varied by shining 1 to 5000 pulses on one spot. After irradiation, the sample was annealed for 1 h at 200°C to remove color centers and other meta-stable laser-induced defects in the glass [13].

The intensity dependence of Ag nanoparticle modification was studied analyzing these irradiated spots in a setup for local transmission spectroscopy, as sketched in Fig. 1(a). By help of the measured, approximately Gaussian intensity distribution of the laser beam, any position within an irradiated spot can be rescaled to the intensity applied in that place. The principle is shown in Fig. 1(b), giving on the left-hand side a projection of the spectrometer entrance slit (rectangle) on the modified spot. Lenses L2 and L3 were chosen so that the slit width of 100 μm was small compared to the size of the (enlarged) spot image, and spectral changes in horizontal direction within the slit were negligible. Since wavelength dispersion is done in the horizontal plane, the (vertical) position r in the slit can thus be correlated to the laser beam intensity in the same position (right-hand side of Fig. 1(b)). Recording the transmitted

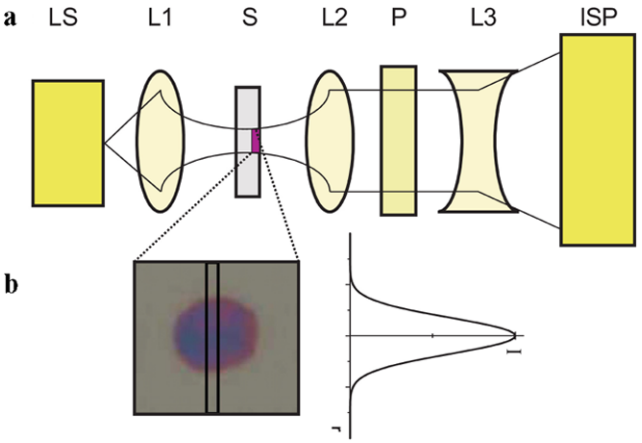

Fig. 1 (**a**) The scheme of the setup for the measurements of spatially resolved transmission spectra. LS—light source, L1, L2, L3—lenses, S—sample, P—polarizer, ISP—imaging spectrometer. (**b**) Enlarged image of modified area and Gaussian intensity profile of the laser beam

light with a CCD camera in the focal plane of the polychromator, intensity-dependent spectra are obtained simultaneously. The spectrometer (ISP) was a Jobin Yvon imaging spectrograph CP140 coupled with a CCD (TE/CCD-1024-EM/EEV30-11/UV from Roper Scientific). The modified areas on the sample were illuminated by a broadband light source (LS). In order to measure polarized transmission spectra, a polarizing prism P was used. The calibration of the image in real sizes was done by a micro scale.

3 Results and interpretation

We have produced various dichroic areas on the sample by irradiating different numbers of laser pulses (ranging from 1 to 5000) to the same spot. The huge number of spectra resulting from the described analysis can only be shown here in a parametrized form (see below). Nonetheless, to demonstrate the quality of the spectra and explain the parametrization, a few examples are shown in Fig. 2. The spectra shown in Figs. 2(a) and (b) were obtained for parameters very similar to our previous work [14, 15], those presented in Figs. 2(c) and (d) at higher intensity. Figures 2(a) and (c) represent the case of multi-shot. Figures 2(b) and (d) that of single shot irradiation. In general, the original SPR band peaked at $\lambda = 413$ nm splits into two polarization dependent bands upon irradiation, but with significant dependence on peak pulse intensity and number of pulses applied. Figure 2(a) shows multi-shot irradiation (1000 pulses at 0.6 TW/cm^2), which produces bands on different sides of the original SPR band: for polarization parallel to that of the laser (p-polarized, blue line), the peak position is shifted to longer wavelengths, while for perpendicular polarization (s-polarized, red line) the band is observed at a shorter wavelength.

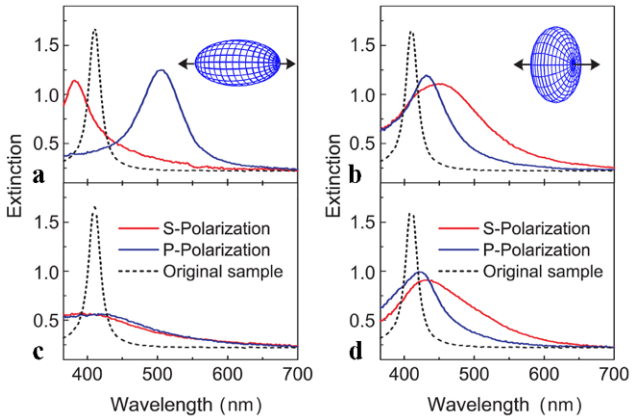

Fig. 2 Polarized extinction spectra of original and irradiated samples: (**a**) multi-shot regime (1000 pulses per spot), peak pulse intensity $I_p = 0.6$ TW/cm^2; (**b**) single shot regime, $I_p = 3$ TW/cm^2; (**c**) multi-shot (5000 pulses per spot), $I_p = 1.2$ TW/cm^2; (**d**) single shot, $I_p = 3.5$ TW/cm^2

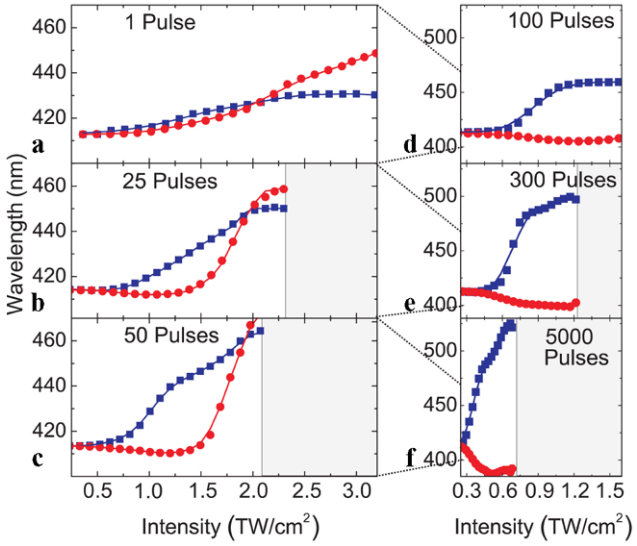

Fig. 3 Dependence of the SP maxima in polarized extinction spectra of soda-lime glass with spherical Ag nanoparticles on laser pulse intensity by irradiation at 400 nm. *Red circles*—s-polarization, *blue squares*—p-polarization, *light gray area*—region of the SP bleaching

This can be explained on the nanoscale by prolate silver spheroids with their symmetry axes oriented along the laser polarization (inset in Fig. 2(a)). In the single-shot case (Fig. 2(b), referring to 3 TW/cm^2), the s-polarized band has a larger red-shift than the p-polarized band. Additionally, both bands are red-shifted in this case. These spectra are due to oblate Ag particles (inset in Fig. 2(b)), again with their symmetry axes oriented along the (horizontal) laser polarization [15]. At even higher intensities and, in particular, in the multi-shot regime, the spectral shifts are becoming smaller and the band integrals decrease. These effects, which are obviously indicating at least partial destruction of the silver nanoparticles, are most clearly seen in Fig. 2(c) (representing 5000 pulses at 1.2 TW/cm^2), but tentatively also in the single-shot regime (Fig. 2(d), 3.5 TW/cm^2).

In general, the examples of Fig. 2 show clearly that the laser-induced shape transformations of Ag nanoparticles and the observable spectral parameters connected with it (orientation of dichroism, peak position and integrated extinction of the SPR bands) are strongly depending on the peak pulse intensity and the number of pulses irradiated to one spot. In order to elucidate the key parameters for the obviously different reshaping mechanisms, we have determined the SP peak central wavelengths as a function of local intensity from various spots irradiated with different number of laser pulses.

These results, a selection of which is presented in parametrized form in Fig. 3, show that laser-induced spectral changes start at intensities of 0.2–0.3 TW/cm^2. For single-shot irradiation (Fig. 3(a)), increase of pulse intensity above this threshold leads to shift of both SP bands towards longer wavelengths. First, in the region of ∼0.3–2 TW/cm^2 one observes a rather weak dichroism, where the p-polarized SP band has the stronger red-sift. At approximately 2 TW/cm^2 the extinction is becoming isotropic again, seen as crossing of the curves for s- and p-polarization at $\lambda = 427$ nm. Above 2 TW/cm^2 a reversed dichroism is observed, i.e., the s-polarization band is now more red-shifted than the p-band. The maximum spectral gap between p- and s-polarized SP bands (peaks at 430 nm and 450 nm, respectively) is found at ∼3.2 TW/cm^2. At still higher intensity beyond 3.2 TW/cm^2 (not shown on the Fig. 3), the SP bands move back toward shorter wavelengths, and the integrated band extinction decreases, indicating (partial) destruction of the silver nanoparticles.

Irradiating 25 pulses to one spot (Fig. 3(b)) we find, in general, a similar peak pulse intensity dependence of the induced dichroism with the two characteristic intensity ranges. There are, however, some important differences compared to the single-shot case: (i) The dichroism (spectral spacing between the polarization dependent bands) is much larger in the low intensity range (below 2 TW/cm^2). (ii) Between 0.3 and 1.3 TW/cm^2 the s-polarized SP band is blue-shifted relative to the original SP peak at 413 nm. (iii) The region of reversed dichroism has shrunk considerably because already from ∼2.3 TW/cm^2 on bleaching of the extinction (particle destruction) starts. In such cases, the analysis of the SP peak central wavelengths was halted (grey regions in Fig. 3).

If the number of pulses irradiated to one spot is further increased one observes that the maximum dichroism grows and is reached at lower peak pulse intensity (Figs. 3(c–f); note the scales change from Figs. 3(c) to (d)). The crossing point of the curves for the p- and s-band, however, remains approximately constant around 2 TW/cm^2, while the region of beginning particle destruction comes down to lower intensity step by step to finally ∼0.7 TW/cm^2 at 5000 pulses

per spot (Fig. 3(f)). Thus, for 100 or more pulses per spot we can only observe the low intensity region of spectral changes with the corresponding dichroism, because following increase of intensity leads to destruction of nanoparticles and results in a bleaching of SP bands. The maximum dichroism recognized in our experiments was found in the case of 5000 pulses, where, at the pulse intensity of 0.65 TW/cm^2, the p- and s-bands are peaked at 525 and 390 nm, respectively. It should be mentioned here that even more than 5000 pulses per spot do not increase the induced dichroism further.

As shown in our previous work [9–13], the principal persistent modifications induced by fs laser pulses do not only comprise the transformation of nanoparticle shapes, but also the generation of a surrounding region of small Ag particles ('halo'). While the first effect explains the splitting of the SP band (dichroism), the second one causes, in a first approximation, a modified matrix refractive index which may lead to isotropic spectral shift of the SP bands [13, 15]. In this work, we have observed both band splitting and spectral shifts as a function of both peak intensity of the fs laser pulses and irradiation density (number of pulses per spot). The first important result was that, independent of the number of pulses applied, there exist two special intensities $I_1 \approx 0.2$ TW/cm^2 and $I_2 \approx 2$ TW/cm^2. For intensities $I < I_1$ there is no spectral change at all, and at $I = I_2$ only spectral shift of the SP band to long wavelengths is observed. In the intensity region $I_1 < I < I_2$, dichroism is found with the larger red-shift for the p-polarized SP band, while for $I > I_2$ a reversed dichroism is seen. This indicates that the processes of shape transformation are controlled by the laser pulse intensity (energy density per pulse), while the number of pulses applied mainly accumulates the changes caused by each single pulse.

Looking in more detail to the low-intensity region $I_1 < I < I_2$ first, the dichroism observed there could be associated with a transformation of the original silver nanospheres into prolate spheroids with their long axis oriented parallel to the laser polarization [12–15]. Anticipating volume conservation for the silver, Mie theory predicts for this case blue- (red-) shift of the SPR of the short (long) particle axis, the spectral spacing between the two bands being correlated to the aspect ratio of the nanoparticle. So the growth of dichroism with increasing number of pulses can be explained by successive increase of the particles' aspect ratio. A red-shift of both bands, however, as observed for 1 pulse for all intensities or at $I > 1.5$ TW/cm^2 at 25 or 50 pulses, can only be explained by additional modification of the host matrix in the vicinity of the nanoparticle which was shown in [13]. So it is obvious to assign the increasing general red-shift for higher pulse intensities to a growing influence of the halo.

In the high-intensity region $I > I_2$, oblate spheroids with their symmetry axes (short axis) along the laser polarization

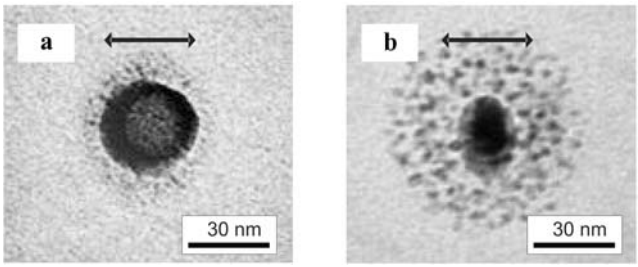

Fig. 4 Transmission Electron Microscopy of Ag nanoparticles in soda-lime glass after irradiation: (**a**) in the region around $I_2 \approx 2$ TW/cm^2, (**b**) partially destructed nanoparticle. Laser polarization is shown as an *arrow*

are produced [14, 15]. Again the fact that both SP bands are red-shifted indicates significant modification of the particle surroundings because otherwise the short axis should show a blue-shifted SP band.

To get an idea about the nanoscopic modifications in the region around $I_2 \approx 2$ TW/cm^2, and in the region of beginning particle destruction (where SP band extinction starts to decrease again), transmission electron microscopy is quite instructive. It should be mentioned, however, that it is not possible to assign an exact local irradiation intensity to a special TEM image. Figure 4 shows two examples for particle shapes found after single-shot irradiation in the high intensity regime [10]; Fig. 4(a) refers to intermediate intensity (around I_2), Fig. 4(b) to very high intensity (significantly above I_2). In the first case, a fairly spherical particle with a limited halo region is seen. In contrast, at very high intensity there is on the one hand a non-spherical central Ag particle, but a much larger region of small silver fragments. Considering that this image was taken after one laser pulse only, it is quite plausible that after several pulses of sufficiently high intensity the particles are destroyed completely and the pertinent SPR band vanishes. In our experiments, total bleaching of the samples has been observed at intensities higher than 1.2 TW/cm^2 applying at least 5000 pulses per spot. We interpret this finding as complete destruction of the Ag nanoparticles into small fragments without distinct SPR.

On the low-intensity side, in particular if one irradiates the sample with many pulses only slightly above the modification threshold (0.2–0.3 TW/cm^2), the maximum spectral shift (and thus the maximum particle aspect ratio) achievable is limited [12] because, due to successive particle deformation, the SP band polarized along the laser polarization moves out of resonance decreasing the interaction with the laser pulses. If higher dichroism is intended in this intensity range, the excitation wavelength has to be tuned to longer wavelengths along with the shift of the SP band [12].

4 Discussion

Before the discussion of the mechanisms leading to the different, intensity dependent shape transformations of silver nanoparticles in glass we want to collect all physical processes, which can occur by the interaction of the laser light with nanoparticles.

A first point to discuss in this context is the temperature rise caused by one laser pulse. Following the intense and resonant laser irradiation, the energy absorbed by the nanoparticles conduction electrons causes a rapid increase in the electronic temperature. Electrons rapidly relax into a quasi-equilibrated hot electron system within several hundreds of femtoseconds [18, 19] via electron–electron scattering. After establishing a thermal electron system, the hot electrons cool down by sharing their energy with the nanoparticles lattice via electron–phonon (e–ph) couplings [19], thereby heating up the particle. The estimations of maximal electronic and lattice temperature for the same system irradiated by pulses with similar intensities were done in [20]. These simplified calculations, based on the Two Temperature Model (TTM), give values in the range of 10^4 K for the electron system and a lattice temperature close to the vaporization temperature for bulk silver. Although the real temperature of a nanoparticle is expected to be lower (because of the nanoparticle energy losses caused by the electron and ion emission, which will be discussed later), one can conclude that in the course of dissipation of the absorbed laser energy the nanoparticles and as a result its immediate surroundings experience a strong transient 'temperature' increase, which is at least connected with strongly enhanced local mobility of electrons, ions and atoms.

Another important effect for our discussion, the photoionization of the silver nanoparticles during exposure to intense fs laser pulses, was recently proven by luminescence experiments [13]. The physical idea is that the SPR enhances the electric field of the laser pulse close to an Ag particle by a few orders of magnitude, with the highest fields located at the poles (with respect to laser polarization) of the nanospheres [21]. This can lead to enhanced directed electron emission from the particle surface [22, 23], preferentially parallel to the laser polarization. But also an isotropic, thermal electron emission has to be regarded in the time of the electron–phonon system thermalization. The anisotropy of the direct, laser-driven electron ejection is thought to provide the preferential direction for the following particle shape transformation. Possibly the high electric field in the vicinity of the metal nanoparticle can even exceed the breakdown threshold of glass resulting in high-density electron plasma formation and even ablation of the glass matrix on the poles of the nanosphere. Regardless whether this happens or not, the free electrons in the matrix will lead to formation of color centers (trapped electrons) in the surroundings of the Ag nanoparticle [13], which should also play an important role for the particle shape modifications. The free electrons as well as the color centers have strong absorption at SP resonance [14] which might result in resonant coupling of SP oscillations to the matrix [24]. Finally, the ionized positively charged core of the Ag nanoparticles is unstable and the Coulomb forces will eject silver cations, which form a cationic shell in the vicinity of the nanoparticle [13]. Clearly the radius of such a cationic shell is determined by the diffusion length of the silver cations and thus strongly depends on the local temperature.

All the effects mentioned above are transient phenomena which are controlled either directly by the electric field of the laser pulse or indirectly by the temperature rise induced by it. Thus, the pulse intensity is doubtless the decisive parameter for the shape transformation of the metal nanoparticles, and it is obvious to assume that the prevalence of individual processes, due to their different intensity dependence, leads to the characteristic intensity regions found in Sect. 3. Based on these qualitative conclusions and the novel information from the complete intensity dependence of laser-induced spectral changes presented above, we suggest the following mechanisms to be mainly responsible for the different shape transformation of silver nanoparticles in soda-lime glass in the different intensity regions.

In the low intensity region, i.e., between $I_1 \approx 0.2$ TW/cm^2 and $I_2 \approx 2$ TW/cm^2, SP field enhancement stimulates the fastest process, field-driven electron emission from the surface of the metal particles (Fig. 5(a)). The emission process happens within a few fs [25], i.e., without delay against the laser pulse. The ejected electrons will then be trapped in the matrix forming color centers close to the poles of the sphere. The ionized nanoparticles are likely to emit Ag ions in statistical directions, in particular when after a few picoseconds electron thermalization and heat transfer to the silver lattice is finished. The resulting positively charged shell of silver cations [13] around the particle meets trapped electrons which are mostly concentrated at the poles. After some picoseconds, when the heat flow coming from the particle increases the electron and ion mobility, they can recombine to Ag atoms (Fig. 5(b)) which finally diffuse back to the nanoparticle and precipitate mainly at the poles. Silver atoms which are situated relatively far away from the main nanoparticle can locally precipitate to each other forming very small clusters. In multi-shot mode, remaining silver ions may also act as trapping centers for the electrons being emitted by the next laser pulse (Fig. 5(c)). Possibly also the fact that electrons are favorably being trapped close to the poles, while ions which are mostly concentrated around equator (because the purely thermal emission of electrons leads to less electrons available for ion annihilation there), may cause local electric field distributions which influence the directional properties of electron and ion emission for following laser pulses. All these processes lead obviously to

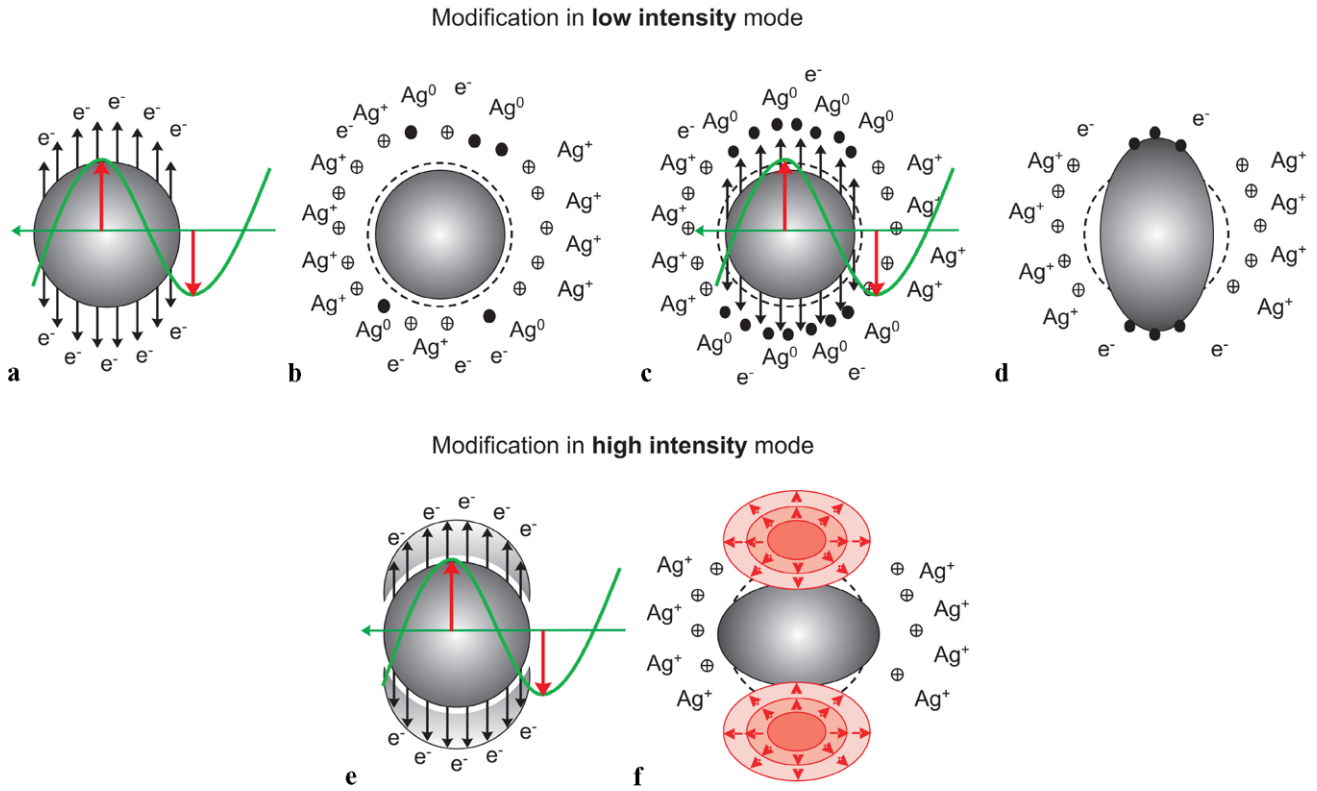

Fig. 5 Laser assisted shape transformation of the metal nanosphere

a step-by-step growth of the Ag particles along the laser polarization, explaining the observed prolate spheroidal shape (Fig. 5(d)). Especially, in the growing process most of the very small silver clusters having precipitated above the poles (defined by the laser polarization) become closer to the main nanoparticle and can be incorporated in it again, while the clusters situated around equator contribute only to the halo formation [15].

With increasing peak pulse intensity we expect higher temperature, thus larger radius of the cationic shell. In this case, the farthest clusters located even in direction of laser polarization cannot diffuse back to the main nanoparticle, and in consequence a larger halo region is observed. This is perfectly compatible with the observed intensity dependence: from typically 1.5 TW/cm^2 on, we observed decreasing dichroism and increasing isotropic red-shift, which can be attributed to the growing influence of the halo (via refractive index increase). It should be mentioned that all the processes discussed require the presence of a rigid, ionic matrix. This may explain why up to now the laser-induced transformation of metal nanoparticles has only been observed in glass nanocomposites.

For the high intensity range above 2 TW/cm^2 we suggest that, in addition to the processes already discussed, the very high local electric field at the poles of the sphere along the laser polarization can accelerate the free electrons so strongly that they induce a high density plasma by avalanche ionization of the glass (Fig. 5(e)). The following plasma relaxation transfers energy from electrons to the lattice (e–ph interaction) on a time scale much faster than the thermal diffusion time. This can finally result in ablation of the material on the interface between glass and metal inclusion leading to partial destruction of the nanoparticle on the poles (Fig. 5(f)), or direct emission of the plasma components further away into the matrix. In any case that process produces oblate rather than prolate particle shapes. It seems very plausible to anticipate that the characteristic intensity producing isotropic spectral changes only ($I_2 \approx 2$ TW/cm^2) marks the balance between (i) the processes leading to particle growth along the laser polarization and (ii) the beginning plasma formation at the particle/matrix interface counteracting this growth.

The final question to be integrated in the picture is that of total particle destruction, which we have observed at intensities above 1.2 TW/cm^2 applying more than 5000 pulses to one spot. It has already been mentioned that heating of the sample for several minutes above 600°C (glass transition temperature) initiates the reformation of spherical particle shapes. Also, preliminary results irradiating heated samples (to be published elsewhere) show that above ∼200°C sample temperature the laser-induced shape transformation is always accompanied by particle destruction. Therefore, we

believe that sufficiently high local temperature (connected with high ion mobility) enables the ejected electrons and ions to move so far away from the nanoparticles that recombination and coalescence are suppressed. Further detailed studies will be necessary to elucidate if local accumulation of heat in the focal volume over a few thousand pulses plays a role in this process, or if just the repeated, transient local heating caused around the Ag particles by each single laser pulse is sufficient to explain destruction.

5 Conclusions

In this study, we have shown that laser induced shape transformation of silver nanoparticles embedded in glass can only be achieved using fs pulses of a minimum peak pulse intensity of 0.2 TW/cm^2. Above this threshold, two main intensity ranges can be distinguished macroscopically by a reversal of the observed dichroism, which is caused by different shapes of the nanoparticles. In the low intensity range (between 0.2 and 2 TW/cm^2), uniformly oriented, prolate spheroids with different aspect ratios are produced, while applying intensities above 2 TW/cm^2 results in oblate spheroids. Directly at 2 TW/cm^2 no dichroism, but only red-shift of the surface plasmon bands is seen, plausibly explained by spherical particles with halo, which have been recognized in TEM images. Increasing the number of pulses increases the induced dichroism for the low intensities and leads to total destruction of the silver nanoparticles for high intensities.

We also proposed the possible deformation mechanisms based on the transient phenomena which are controlled either directly by the electric field of the laser pulse or indirectly by the temperature rise induced by it. Formation of the prolate spheroids with the long axis parallel to the laser polarization in the low intensity range for multi-shot irradiation could be explained by combination of the photoionization and metal particle precipitation on the poles of the nanosphere. The intensity-dependent extension of the cationic shell around the nanoparticle and the photoelectron emission in direction of the laser polarization play a key role here. In the case of high intensities (above 2 TW/cm^2) and low number of pulses (less then 40), dense electron plasma formation at the poles of the sphere and following thermal expansion or even ablation of the glass matrix dominate, leading to transformation of nanospheres to oblate spheroids.

Acknowledgements The authors thank H. Hofmeister for the TEM images, CODIXX AG for the samples and the Deutsche Forschungsgemeinschaft for financial support through SFB 418.

References

1. U. Kreibig, M. Vollmer, *Optical Properties of Metal Clusters* (Springer, Berlin, 1995)
2. V.M. Shalaev, *Optical Properties of Nanostructured Random Media* (Springer, Berlin, 2001)
3. P.J. Chakraborty, Mater. Sci. **33**, 2235 (1998)
4. R. Jin, Y.W. Cao, C.A. Mirkin, K.L. Kelly, G.C. Schatz, J.G. Zheng, Science **249**, 1901 (2001)
5. T. Wenzel, J. Bosbach, A. Goldmann, F. Stietz, F. Träger, Appl. Phys. B **69**, 513 (1999)
6. F. Stietz, Appl. Phys. A **72**, 381 (2001)
7. A.L. Stepanov, D.E. Hole, A.A. Bukharaev, P.D. Townsend, N.I. Nurgazizov, Appl. Surf. Sci. **136**, 298 (1998)
8. A.L. Stepanov, V.N. Popok, Surf. Coat. Technol. **185**, 30 (2004)
9. M. Kaempfe, T. Rainer, K.-J. Berg, G. Seifert, H. Graener, Appl. Phys. Lett. **74**, 1200 (1999)
10. M. Kaempfe, G. Seifert, K.-J. Berg, H. Hofmeister, H. Graener, Eur. Phys. J. D **16**, 237 (2001)
11. G. Seifert, M. Kaempfe, K.-J. Berg, H. Graener, Appl. Phys. B **73**, 355 (2001)
12. A. Podlipensky, A. Abdolvand, G. Seifert, H. Graener, Appl. Phys. A **80**, 1647 (2005)
13. A. Podlipensky, V. Grebenev, G. Seifert, H. Graener, J. Lumin. **109**, 135 (2004)
14. A.V. Podlipensky, PhD thesis, Martin-Luther Universität Halle-Wittenberg, 2005. http://sundoc.bibliothek.uni-halle.de/diss-online/05/05H084/t1.pdf
15. A. Stalmashonak, G. Seifert, H. Graener, Opt. Lett. **32**, 3215 (2007)
16. K.-J. Berg, A. Berger, H. Hofmeister, Z. Phys. D **20**, 309 (1991)
17. D. Du, X. Liu, G. Mourou, Appl. Phys. B **63**, 617 (1996)
18. N. Del Fatti, C. Voisin, M. Achermann, S. Tzortzakis, D. Christofilos, F. Vallee, Phys. Rev. B **61**, 16956 (2000)
19. J.Y. Bigot, V. Halte, J.C. Merle, A. Daunois, Chem. Phys. **251**, 181 (2000)
20. A.A. Unal, A. Stalmashonak, G. Seifert, H. Graener, Proc. SPIE **7032**, 703225 (2008)
21. K.L. Kelly, E. Coronado, L.L. Zhao, G.C. Schatz, J. Phys. Chem. B **107**, 668 (2003)
22. A. Akella, T. Honda, A.Y. Liu, L. Hesselink, Opt. Lett. **22**, 967 (1997)
23. W. Pfeifer, C. Kennerknecht, M. Merschdorf, Appl. Phys. A **78**, 1011 (2004)
24. A. Melikyan, H. Minassian, Appl. Phys. B **78**, 453 (2004)
25. F. Calvayrac, P.G. Reinhard, E. Suraud, C.A. Ullrich, Phys. Rep. **337**, 493 (2000)